



**HAL**  
open science

## Monoclonal antibodies reveal the alteration of the rhodocetin structure upon alpha2beta1 integrin binding

Thilo Bracht, Flavia Figueiredo de Rezende, Jörg Stetefeld, Lydia M Sorokin, Johannes A Eble

### ► To cite this version:

Thilo Bracht, Flavia Figueiredo de Rezende, Jörg Stetefeld, Lydia M Sorokin, Johannes A Eble. Monoclonal antibodies reveal the alteration of the rhodocetin structure upon alpha2beta1 integrin binding. *Biochemical Journal*, 2011, 440 (1), pp.1-11. 10.1042/BJ20110584 . hal-00642833

**HAL Id: hal-00642833**

**<https://hal.science/hal-00642833>**

Submitted on 19 Nov 2011

**HAL** is a multi-disciplinary open access archive for the deposit and dissemination of scientific research documents, whether they are published or not. The documents may come from teaching and research institutions in France or abroad, or from public or private research centers.

L'archive ouverte pluridisciplinaire **HAL**, est destinée au dépôt et à la diffusion de documents scientifiques de niveau recherche, publiés ou non, émanant des établissements d'enseignement et de recherche français ou étrangers, des laboratoires publics ou privés.

## Monoclonal antibodies reveal the alteration of the rhodocetin structure upon $\alpha 2\beta 1$ integrin binding

Thilo Bracht<sup>\*</sup>, Flávia Figueiredo de Rezende<sup>\*</sup>, Jörg Stetefeld<sup>†</sup>, Lydia M. Sorokin<sup>‡</sup>, Johannes A. Eble<sup>\*§</sup>

<sup>\*</sup>Excellence Cluster Cardio-Pulmonary System, Center for Molecular Medicine, Vascular Matrix Biology, Frankfurt University Hospital, Frankfurt/Main, Germany; <sup>†</sup>Departments of Chemistry and Microbiology, University of Manitoba, Winnipeg R3T 2N2, MB, Canada

<sup>‡</sup>Institute of Physiological Chemistry and Pathobiochemistry, University of Münster, Münster, Germany

**Short title:** Heterotetrameric rhodocetin dissociates upon  $\alpha 2\beta 1$  integrin binding.

§ corresponding author:

Johannes A. Eble

Center for Molecular Medicine

Dept. Vascular Matrix Biology

Frankfurt University Hospital

Building 9

Theodor-Stern-Kai 7

60590 Frankfurt/Main

Germany

Phone: +49-69-6301 87651

Fax: +49-69-6301 87656

E-mail: [Eble@med.uni-frankfurt.de](mailto:Eble@med.uni-frankfurt.de)

**SYNOPSIS:**

The  $\alpha 2\beta 1$  antagonist rhodocetin from *Calloselasma rhodostoma* is a heterotetrameric C-type lectin-related protein (CLRP) consisting of four distinct chains,  $\alpha$ ,  $\beta$ ,  $\gamma$ , and  $\delta$ . Via their characteristic domain-swapping loops, the individual chains form two subunits,  $\alpha\beta$  and  $\gamma\delta$ . To distinguish the four chains which share similar molecular masses and high sequence homologies, we generated 11 monoclonal antibodies (mAbs) with different epitope specificities. Four groups of distinct mAbs were generated: the first targeted the rhodocetin  $\beta$  chain, the second group bound to the  $\alpha\beta$  subunit mostly in a conformation-dependent manner, and the third group recognized the  $\gamma\delta$  subunit only when separated from the  $\alpha\beta$  subunit, while a fourth group interacted with the  $\gamma\delta$  subunit both in the heterotetrameric molecule and complexed with the integrin  $\alpha 2$  A-domain. Using the specific mAbs, we showed that the rhodocetin heterotetramer dissociates into the  $\alpha\beta$  and  $\gamma\delta$  subunit upon binding to the integrin  $\alpha 2$  A-domain at both molecular and cellular levels. After dissociation, the  $\gamma\delta$  subunit firmly interacts with the  $\alpha 2\beta 1$  integrin thereby blocking it, while the rhodocetin  $\alpha\beta$  is released from the complex. The small molecular interface between the  $\alpha\beta$  and  $\gamma\delta$  subunit within rhodocetin is mostly mediated by charged residues, which renders the two dissociated subunits with hydrophilic surfaces.

**KEYWORDS:**

C-type lectin-like protein (CLRP); venom;  $\alpha 2\beta 1$  integrin; rhodocetin; quaternary structure; dissociation

**ABBREVIATIONS:**

mAb, monoclonal antibody; CLRP, C-type lectin-related protein;

## INTRODUCTION:

Integrin  $\alpha 2\beta 1$  is a collagen receptor that is widely expressed on different cell types, such as fibroblast, epidermal and endothelial cells, and platelets [1]. As member of the integrin family [2], it consists of two genetically non-related subunits,  $\alpha 2$  and  $\beta 1$ , the latter one of which is shared with most extracellular matrix binding integrins. The extracellular domains of both integrin subunits shape the head domain which harbors the ligand interaction site. Within their  $\alpha$  subunits, the collagen-binding integrins contain an additional A-domain, which is also located within the head region. The integrin  $\alpha 2$  A-domain is crucially involved in collagen binding [3, 4]. Upon collagen binding, it undergoes a substantial conformational change, which is conveyed through the entire molecule to the cytoplasmic tails. Thus, environmental cues from the extracellular matrix are transduced into the cells in the outside-in signaling process of integrins [5]. Consequently, several  $\alpha 2\beta 1$  integrin-related functions are triggered upon cell attachment to collagen, such as force transmission, migration and expression of both collagens and collagen-degrading proteases [6-10]. Moreover,  $\alpha 2\beta 1$  integrin is the major collagen-binding integrin on platelets, although GP VI on platelets also binds collagen [11]. The role of  $\alpha 2\beta 1$  integrin versus GPVI in collagen-induced platelet activation and aggregation is therefore still controversially discussed [12-14]. Due to the redundancy of collagen receptors [11] and compensatory mechanisms by other collagen-binding integrins [15, 16], the genetic ablation of the integrin  $\alpha 2$  subunit in mice results in a subtle phenotype, which includes reduced collagen-induced platelet aggregation [17-19]. In addition to thrombosis, integrin  $\alpha 2\beta 1$  plays an important role in several physiological and pathological processes, such as wound healing and fibrosis [6]. Hence, a search for  $\alpha 2\beta 1$  integrin-targeting pharmaceuticals has been initiated [20, 21].

The importance of  $\alpha 2\beta 1$  integrin in collagen-induced platelet aggregation probably contributed to its evolution into a natural target for hemorrhagic venoms, such as from snakes. A common recognition motif that is mimicked by disintegrins in numerous snake venoms is the peptide sequence RGD [22]. However,  $\alpha 2\beta 1$  integrin binds to collagen in an RGD-independent manner and rather requires a 6 amino acids, GFPGER, which must be presented in a collagenous triple helix [8, 23, 24]. So far, three naturally occurring inhibitors of  $\alpha 2\beta 1$  integrin have been identified from snake venoms: rhodocetin from *Calloselasma rhodostoma* [25], EMS16 from *Echis multisquamatus* [26], and VP12 from *Vipera palestina* [27]. All three toxins lack a collagenous triple-helical domain. They belong to the family of C-type lectin-related proteins (CLRPs), for which the name 'snake venom C-type lectins' or 'snaclecs' has been coined [28, 29].

Rhodocetin was originally described as heterodimer consisting of two chains,  $\alpha$  and  $\beta$  [25, 30], that associate firmly, but non-covalently, via a loop exchange motif typical for CLRPs from snake venoms [31, 32]. Due to similar molecular masses and high homology of the rhodocetin chains it was subsequently realized that rhodocetin not only consists of two, but of four distinct chains,  $\alpha$ ,  $\beta$ ,  $\gamma$ , and  $\delta$ , which exist in two heterodimeric subunits,  $\alpha\beta$  and  $\gamma\delta$ , to form a unique quaternary structure [33]. In previous studies, we also previously demonstrated that rhodocetin strongly interacts with the integrin  $\alpha 2$  A-domain, thereby blocking collagen binding to  $\alpha 2\beta 1$  integrin and that it antagonizes  $\alpha 2\beta 1$  integrin-mediated cellular functions in different cell systems [34, 35]. Here, we have developed monoclonal antibodies (mAbs) against rhodocetin and its subunits, to precisely define the molecular mechanism of rhodocetin's action. Being specifically directed against the individual subunits, these mAbs not only confirm the heterotetrameric nature of rhodocetin, but are also ideal tools to monitor the fate of the individual rhodocetin subunits during integrin binding. We demonstrate that the heterotetrameric rhodocetin dissociates upon binding to  $\alpha 2\beta 1$  integrin, which is likely to be accompanied by conformational changes within the rhodocetin subunits. The rhodocetin  $\gamma\delta$  subunit firmly binds to the  $\alpha 2\beta 1$  integrin, while the rhodocetin  $\alpha\beta$  subunit is released from

the complex and acts as an independent entity. Moreover, rhodocetin dissociates not only in protein interaction assays, but also under physiological conditions after it has bound to the membrane-anchored  $\alpha 2\beta 1$  integrin on cells.

## EXPERIMENTAL:

### *Reagents:*

Tetrameric rhodocetin was purified and its subunits were separated as described previously [33]. Recombinant integrin  $\alpha 2$  A-domain [33] was allowed to form a complex with the rhodocetin  $\gamma\delta$  subunit as described elsewhere [36]. A polyclonal antiserum against tetrameric rhodocetin was raised in rabbit according to standard protocols. It recognized all four subunits of rhodocetin in ELISA and Western blot, both with and without reduction of the antigen.

The cDNA, which encodes the fusion protein of His-tagged integrin  $\alpha 2$  A-domain with enhanced yellow fluorescent protein (EYFP), was generated in two PCR steps. The part of cDNA encoding the N-terminal oligoHis- $\alpha 2$  A-domain was amplified from pET15b- $\alpha 2A$  [33] using primers containing an NcoI and an AgeI restriction site at the 5'- and 3'-end, respectively. Likewise, the EYFP sequence was amplified from pIRES-EYFP (Clontech Laboratories, Palo Alto, CA, USA) using primers containing AgeI and NdeI sites at the 5'- and 3'-end, respectively. Subsequently, both amplicons were ligated with their AgeI sites into the pET15b which was previously digested with NcoI and NdeI. Finally, the construct pET15b- $\alpha 2A$ -YFP was verified by sequencing. *E. coli* BL21(DE3) bacteria transformed with this plasmid by electroporation produced the recombinant fusion protein called  $\alpha 2A$ -YFP. It was purified by metal ion affinity chromatography using NiNTA column (GE Healthcare, Munich, Germany) and detected by its fluorescence at 527 nm after excitation at 514 nm.

### *Immunization of mice and rats and generation of monoclonal antibodies:*

Two Balb/c mice and two Sprague Dawley rats were used for immunizations. Tetrameric rhodocetin was subcutaneously injected into a mouse (first fusion), the isolated rhodocetin  $\gamma\delta$  subunit into another mouse and a rat (second and third fusion, respectively), and the complex of rhodocetin  $\gamma\delta$  with the integrin  $\alpha 2$  A-domain into another rat (fourth fusion). The antigens were applied together with complete and incomplete Freund's adjuvants in the first and the subsequent immunization injections, respectively. The splenic lymphocytes were fused with a three-fold surplus of SP2/0 myeloma as described previously [37]. Conditioned media from hybridomas were tested for antibody production by ELISA and isolated into single cell-derived clones in two subsequent rounds of subcloning.

### *ELISA for hybridoma screening and for titration assays:*

Not only the antigens used for immunization (tetrameric rhodocetin, rhodocetin  $\gamma\delta$ , and rhodocetin  $\gamma\delta$ -integrin  $\alpha 2$  A-domain complex), but also the other isolated rhodocetin subunits and the integrin  $\alpha 2$  A-domain were coated to microtiter plates at 2  $\mu\text{g}/\text{ml}$  in TBS, pH 7.4 overnight at 4°C. After washing twice with TBS and blocking with 1 % BSA-solution in TBS, pH 7.4, containing 1 mM  $\text{MgCl}_2$ , the wells were incubated with hybridoma conditioned media (for hybridoma screening) or purified mAbs (as positive controls at 1  $\mu\text{g}/\text{ml}$  or for titration experiments) in 1% BSA in TBS, pH 7.4,  $\text{MgCl}_2$  for 90 min at room temperature. Bound mAbs were detected with secondary alkaline phosphatase-conjugated antibodies against mouse or rat antibodies diluted to 1:1000 in the same buffer for 90 min. Binding was quantified by conversion of *p*-nitrophenyl-phosphate (Sigma, Deisenhofen, Germany). After stopping the conversion with 1.5 M NaOH solution, absorbance was measured at 405nm in an ELISA reader (Synergy HT, BioTek, Bad Friedrichshall, Germany). Non-specific binding to BSA-coated wells was subtracted from the measured signals. The ELISA was performed in quadruplets.

*Western Blot:*

Two  $\mu\text{g}$  of rhodocetin were electrophoretically separated by SDS-PAGE in a 12-18 % polyacrylamide gel with and without prior reduction and blotted onto nitrocellulose membrane. After blocking with TBST (0.05 % Tween in TBS, pH 7.4), supplemented with 2 % BSA, the membranes was incubated with 2  $\mu\text{g}/\text{ml}$  mAb and rabbit antiserum against rhodocetin (diluted 1:2000), washed with TBST, and incubated with Alexa488-labelled secondary antibodies against murine, rat or rabbit antibodies (Invitrogen, Karlsruhe, Germany). After two washes with TBST and TBS, the stained bands were detected with an Ettan DIGE fluorescence reader (GE Healthcare).

*Antibody interference assay:*

The detecting mAbs were biotinylated with a 25 to 500 molar excess of EZ-Link Sulfo-NHS-LC-Biotin (Pierce, Thermo Scientific, Langensiebold, Germany) in 1 ml PBS (20 mM sodium phosphate, pH 7.4, 150 mM NaCl) for 1 h at room temperature. Biotinylation was stopped by adding 40 mM TRIS/HCl, pH 7.4. Excess biotinylation reagent was removed by dialysis. For the mAb interference assay, 2  $\mu\text{g}/\text{ml}$  rhodocetin tetramer or  $\gamma\delta$  subunit were coated to a microtiter plate in TBS, pH 7.4, overnight at 4°C. After washing and blocking with 1 % BSA, TBS, pH 7.4, 1 mM  $\text{MgCl}_2$ , wells were incubated with each biotinylated, detecting mAb at 1  $\mu\text{g}/\text{ml}$  in the same buffer in the absence or presence of non-biotinylated, interfering mAbs. Bound detecting mAbs were quantified in an ELISA with alkaline phosphatase-conjugated ExtrAvidin (Sigma-Aldrich, Deisenhofen, Germany), diluted 1:1000 in 1 % BSA, TBS, pH 7.4, 150 mM NaCl, 1 mM  $\text{MgCl}_2$ . Conversion of phosphatase substrate was colorimetrically detected in a microtiter plate reader. The signals were corrected for background values, measured in BSA-coated wells, and normalized to the non-inhibited controls, measured in the absence of any interfering mAb. The experiment was carried out in duplicates.

*mAb-inhibition test:*

To test the potential of mAbs to inhibit the binding of rhodocetin to the  $\alpha 2\beta 1$  integrin, the integrin  $\alpha 2$  A-domain was immobilized to the microtiter plate at 10  $\mu\text{g}/\text{ml}$ . After washing and blocking with 1% BSA, rhodocetin was added at increasing concentrations in both the absence and presence of the murine or rat mAb, in at least a 2-fold molar excess. Bound rhodocetin was fixed with 2.5 % glutaraldehyde in 25 mM HEPES, pH 7.4, 150 mM NaCl, 2 mM  $\text{MgCl}_2$ , for 10 min and detected in an ELISA using the rabbit antiserum against rhodocetin.

*Immunoprecipitation of rhodocetin:*

Twenty mg of crude *Calloselasma rhodostoma* venom (Sigma-Aldrich) were dissolved in PBSE (20 mM sodium phosphate, pH 7.4, 150 mM NaCl, 5 mM EDTA), supplemented with leupeptin, pepstatin, aprotinin (each at 1  $\mu\text{g}/\text{ml}$ ), phenanthroline and PMSF (each 1 mM). 100  $\mu\text{g}$  of each mAb (including species-matched control antibodies) were incubated with 30  $\mu\text{l}$  of this crude venom solution in 1 % BSA, PBS, pH 7.4 at a final volume of 300  $\mu\text{l}$  for 2 h at room temperature. 50  $\mu\text{l}$  of equilibrated protein G-beads (Pierce, Thermo Scientific) were added and incubation was continued for another 90 min. Beads were washed three times with PBS, suspended and boiled in SDS-PAGE sample buffer without  $\beta$ -mercaptoethanol, electrophoretically separated by SDS, blotted onto a nitrocellulose membrane, stained with the rabbit antiserum against rhodocetin and fluorescently detected with an Alexa488-labelled secondary antibody as described above.

*Analytical size exclusion chromatography of rhodocetin:*

Rhodocetin (50  $\mu\text{g}$ ), either alone or in an equimolar ratio with YFP-tagged integrin  $\alpha 2$  A-domain (40  $\mu\text{g}$ ), was cross-linked with 1 mM BS3 (Pierce, Thermo Scientific) for 1 h at 26 °C in PBS, pH 7.4, supplemented with 1 mM  $\text{MgCl}_2$ . The cross-linking reaction was stopped with 20 mM TRIS/HCl, pH 7.4 and proteins were separated on a TSK 2000 GWXL column (TosoHass, Stuttgart, Germany) in PBS at 0.5 ml/min. Elution of proteins was monitored by measuring absorbance at 219 nm and fluorescence at 527nm (excitation at 514 nm). The eluate fractions were further analyzed in the rhodocetin subunit-sandwich ELISA.

*Rhodocetin subunit-sandwich ELISA:*

The mAbs VIIG2 and IC3 were coated at 5  $\mu\text{g}/\text{ml}$  in TBS at 4 °C overnight. The microtiter plate was subsequently washed with TBS, pH 7.4, and blocked with 1 % BSA in TBS, pH 7.4, 1 mM  $\text{MgCl}_2$ , before the gel filtration fractions were applied in a 1:100 dilution for 90 min. Captured rhodocetin was quantified with the rabbit antiserum against rhodocetin and an alkaline phosphate-conjugated secondary antibody, both diluted 1:2000, as described above.

*Kinetic surface plasmon resonance measurements:*

The oligo-His-free integrin  $\alpha 2$  A-domain was covalently immobilized to a CM5 chip (GE Healthcare, Freiburg, Germany) according to the manufacturer's instructions. Using BiaCore X (GE Healthcare), sensograms were recorded while solutions of different concentrations of rhodocetin tetramer or rhodocetin  $\gamma\delta$  subunit in 50 mM HEPES/NaOH, pH 7.5, 150 mM NaCl, 1 mM  $\text{MgCl}_2$ , were flown over the integrin  $\alpha 2$  A-domain-coated CM5 chip. The firmly attached rhodocetin molecules were washed off with 50 mM DTT in 50 mM TRIS/HCl, pH 9.5, 300 mM NaCl after every binding cycle. The rhodocetin  $\gamma\delta$  subunit was dissolved as stock solution in the acetonitrile-containing buffer of the reversed phase purification. Hence, correspondingly diluted buffer controls were performed and the respective sensograms were subtracted. The sensograms were assessed with the BIAevaluation v3.1 software (GE Healthcare).

*Flow cytometry:*

$1 \times 10^5$  HT1080 cells were incubated with 2  $\mu\text{g}/\text{ml}$  rhodocetin in PBS, pH 7.4, containing 2 % BSA and 1 % horse serum. After two washes with cold PBS, cells were incubated with mAbs directed against rhodocetin or species-matched control antibodies, each at 2  $\mu\text{g}/\text{ml}$ . Bound murine and rat mAbs were detected with phycoerythrin-conjugated and Alexa568-labelled secondary antibodies against anti mouse IgG and anti rat IgG, respectively, in a CyFlowSL (Partec, Münster, Germany) with  $1 \times 10^4$  events counted per sample.

**RESULTS:***Generation of monoclonal antibodies against rhodocetin and the integrin  $\alpha 2$  A domain-rhodocetin  $\gamma\delta$  complex*

11 stable hybridomas were generated that produced mAbs against rhodocetin. These included nine murine mAbs (VIIG2, VD10, IIIB6, VIIF4, VIIF9, IXH7, VIIB9, IIIG5, and IIC9), all of which were IgG1, and two rat mAbs, IC3 and ID10, that were IgG2a and IgG1, respectively (Supplementary Fig. S1). Three rat hybridomas were obtained which produced mAbs (VIII A8, XD8, and VIH7) against the integrin  $\alpha 2$  A-domain. The IgG2 VIII A8, and the two IgMs XD8 and VIH7, were difficult to purify without loss of activity. They are therefore not subject of this work.

### *Specificity of the newly generated mAbs against rhodocetin:*

The specificities of the murine and rat mAbs were determined in an ELISA, in which the tetrameric rhodocetin, its individual  $\alpha$  and  $\beta$  chains, its subunits  $\alpha\beta$  and  $\gamma\delta$ , its complex with the integrin  $\alpha 2$  A-domain or the integrin  $\alpha 2$  A-domain alone were employed as substrates (Fig. 1). The 9 murine and 2 rat mAbs recognized the individual rhodocetin subunits differently and were sorted into four subgroups. The first subgroup comprised the murine mAbs VIIG2 and VD10 which recognized the rhodocetin  $\beta$  subunit, irrespective of whether it was coated alone or as the rhodocetin  $\alpha\beta$  dimer. By contrast, the murine mAbs IIIB6, VIIF4, and VIIF9, constituting the second subgroup of mAbs, recognized the rhodocetin  $\alpha\beta$  dimeric subunit only, but not  $\alpha$  or  $\beta$  chains alone. A similar antigen recognition behavior was observed for the mAbs directed against the rhodocetin  $\gamma\delta$  subunit. Whereas the mAbs, IXH7, VIIIB9 and IIIG5 bound preferentially to the rhodocetin  $\gamma\delta$  subunit, but not the entire rhodocetin tetramer (third subgroup of mAbs), the mAbs IIC9 from mouse and ID10 from rat showed greater binding to the rhodocetin  $\alpha\beta\gamma\delta$  tetramer than to the rhodocetin  $\gamma\delta$  subunit. The rat mAb IC3 recognized both rhodocetin tetramer and rhodocetin  $\gamma\delta$  subunit equally well. The latter three mAbs, IIC9, ID10 and IC3 form the fourth subgroup of antibodies, which also detect the complex of the rhodocetin  $\gamma\delta$  subunit with the integrin  $\alpha 2$  A-domain, without interacting with the integrin binding partner of rhodocetin.

### *The mAbs VIIG2, VD10, and IIIG5 recognize a sequence epitope*

To distinguish whether the mAbs recognize a conformational or sequence epitope, immunoblots were carried out, in which the electrophoretically separated rhodocetin subunits, both without and with prior reduction (left and right lanes, respectively, in Supplementary Fig. S2) were blotted onto nitrocellulose membranes and probed with the test mAb and the polyclonal rabbit antiserum against rhodocetin. Whereas the two mAbs, VIIG2 and VD10, recognized both the non-reduced and reduced rhodocetin  $\beta$  chain, the other anti- $\beta$  subunit mAb IIIB6 recognized only the non-reduced rhodocetin  $\beta$  chain. The mAb IIIB6 seemed to recognize a certain folding pattern within the rhodocetin  $\beta$  chain. This was further corroborated by the fact that IIIB6 shows a binding signal in ELISA only if the conformation of the  $\beta$  chain is preserved within the  $\alpha\beta$  dimeric subunit or the entire tetrameric rhodocetin molecule (Fig. 1). A similar conformational epitope restriction in Western blot was seen for the mAbs, VIIIB9, IC3 and ID10, all of which exclusively recognized the non-reduced rhodocetin  $\gamma\delta$  subunit. Moreover, they also recognized the disulfide-linked  $(\gamma\delta)_2$  subunit dimers, which run at an apparent molecular mass of 55 kDa in SDS-PAGE. The mAb IIIG5 was the only antibody that detected a sequence epitope within the rhodocetin  $\gamma$  chain, which is exposed only after reductive separation of the rhodocetin  $\gamma$  chains.

### *The affinities of mAbs towards rhodocetin and the effect of rhodocetin $\gamma\delta$ -directed mAbs on rhodocetin-integrin interaction*

The affinities of mAbs towards their antigen were determined by titration of rhodocetin or its respective subunit in an ELISA (Fig. 2A). The titration curves were approximated by a linearization algorithm developed by Heyn and Weischet [38]. The  $K_d$  values calculated by this approximation are summarized in Table I and range from 0.5 nM (VD10) to almost 700 nM (IIIG5).

As the rhodocetin  $\gamma\delta$  subunit contains the binding site for the integrin  $\alpha 2$  A-domain, the  $\gamma\delta$  subunit-targeting mAbs IIC9, IC3 and ID10 were tested for their ability to inhibit the interaction of rhodocetin with the integrin binding domain. Although the titration curves of rhodocetin to immobilized  $\alpha 2$  A-domain were shifted to higher rhodocetin concentrations in the presence of mAbs (Fig. 4B), thus indicating increased  $K_d$ -values (IIC2:  $4.2 \pm 0.4$  nM; IC3:

$6.9 \pm 0.3$  nM; ID10:  $5.7 \pm 0.2$  nM vs.  $2.7 \pm 0.1$  nM in the absence of mAb), none of the three mAbs were able to abrogate the binding of rhodocetin to the  $\alpha 2$  A-domain.

*Epitope specificity of the anti-rhodocetin mAbs:*

To determine whether the newly generated mAbs have overlapping epitope specificities, we performed antibody interference assays. To distinguish the detecting mAb from the interfering mAbs, we biotinylated the detecting mAbs with an amine-reactive biotinylation reagent. Biotinylated detecting mAbs against rhodocetin were allowed to bind to immobilized rhodocetin in the absence and presence of various concentration of an interfering, non-biotinylated mAb. When binding of the biotinylated mAb was compromised by the other mAb, the two mAbs were assigned to same competition group and possess an overlapping or even identical epitope within the rhodocetin molecule. Representative interference curves for VIIG2 and VD10 (Fig. 3A) and for IIC9 (Fig. 3B) are shown as examples with mAbs directed against the  $\alpha\beta$  and  $\gamma\delta$  subunit, respectively. Comprehensive interference tables of anti-rhodocetin  $\alpha\beta$ - and anti rhodocetin  $\gamma\delta$ -mAbs (Figs. 3C and D, respectively) summarize the results. Probably due to sterical hindrance, VIIG2 and VD10, VIIF4 and VIIF9, IXH7 and VIIIB9, IIC9 and ID10 excluded each other mutually from binding to rhodocetin (Fig. 3C and D). Rather than being inhibitory, the mAbs IIIB6, VIIF4, and VIIF9 enhanced binding of the mAbs, VIIG2 and VD10. Interestingly, all the former mAbs recognized the  $\alpha\beta$  heterodimer but not the individual  $\alpha$  or  $\beta$  chain, whereas the latter recognized a sequence epitope within the rhodocetin  $\beta$  chain. Moreover, albeit belonging to the same Ab group, the binding intensity of IIIB6 was increased in the presence of VIIF4 and VIIF9. The enhanced binding signals suggests conformational changes within rhodocetin. Thus, binding of one mAb leads to a conformational change within the rhodocetin molecule, thereby generating the conformational epitope or unmasking the epitope of the other antibody. Within the group of antibodies recognizing the rhodocetin  $\gamma\delta$  subunit, only one positive interference was observed (Fig. 3B and D). IC3 supported the binding of the detecting IIC9 strongly, whereas a reciprocal activation was not observed. Interestingly, such a reciprocal activation did not occur between the rhodocetin  $\alpha\beta$  subunit-recognizing antibodies (Fig. 3C).

*The tetrameric rhodocetin dissociates into its  $\alpha\beta$  and  $\gamma\delta$  subunits upon mAb binding*

To study the interaction of mAbs with rhodocetin in solution, we performed immunoprecipitation experiments (Fig. 4A). All mAbs directed against the rhodocetin  $\beta$  chain, VIIG2, VD10, IIIB6, VIIF4 and VIIF9, precipitated the rhodocetin  $\alpha$  and  $\beta$  chains. However, the precipitates contained hardly any rhodocetin  $\gamma\delta$  subunit. Complementarily, the mAbs, IIC9, IC3 and ID10, directed against the rhodocetin  $\gamma\delta$  subunit preferentially pulled down the  $\gamma\delta$  subunit, with a much smaller amount of accompanying rhodocetin  $\alpha\beta$  subunit. This observation suggested that our mAbs against rhodocetin induced a dissociation of the rhodocetin tetramer into the  $\alpha\beta$  and  $\gamma\delta$  subunits after binding their respective epitopes. Rhodocetin is a heterotetrameric protein in solution and dissociates only after being bound by the antibodies. In support of this hypothesis, the mAbs against rhodocetin  $\gamma\delta$  subunit, IXH7, VIIIB9 and IIIG5, which only recognize their epitopes within the isolated rhodocetin  $\gamma\delta$  subunit but not in the entire tetrameric rhodocetin molecule (Fig. 2), failed to precipitate any rhodocetin chain. However, when the precipitations with these mAbs were carried out in the presence of the anti-rhodocetin  $\beta$ -subunit mAb VIIG2, they pulled down the rhodocetin  $\gamma\delta$  subunit completely (Fig. 4B). This suggests that their epitopes within the rhodocetin  $\gamma\delta$  subunit are masked by the rhodocetin  $\alpha\beta$  subunit and become accessible only after dissociation of the rhodocetin tetramer into its two heterodimeric subunits.

### *Dissociation of rhodocetin upon $\alpha 2$ A-domain binding*

To determine whether the dissociation of the heterotetrameric rhodocetin into its  $\alpha\beta$  and  $\gamma\delta$  subunits is only artificially induced by the mAbs, or whether it represents a physiological process, we performed analytical size exclusion chromatography of rhodocetin without and with its target molecule, the integrin  $\alpha 2$  A-domain. To avoid dissociation of the rhodocetin subunits during gel filtration, we cross-linked rhodocetin with the homo-bifunctional cross-linker BS<sup>3</sup> prior to the size exclusion chromatography. The subunits of rhodocetin in the eluate fractions were identified by sandwich-ELISAs, in which the immobilized mAbs, VIIG2 and IC3, specifically captured the rhodocetin  $\alpha\beta$  or  $\gamma\delta$  subunit, respectively. On the gel filtration column, rhodocetin separated into two major peaks, *I* and *II* (Fig. 5A). Peak *I* with an apparent molecular mass of  $72.3 \pm 1.4$  kDa represented the heterotetrameric rhodocetin molecule with a higher molecular mass shoulder at 108 kDa, which is likely to represent disulfide-linked rhodocetin ( $\gamma\delta$ )<sub>2</sub> including associated  $\alpha\beta$  subunit(s). Peak *II* contained dissociated rhodocetin  $\alpha\beta$  and  $\gamma\delta$  subunits with an apparent molecular mass of  $36.3 \pm 2.0$  kDa. As analysed by Sandwich-ELISA and immunoblotting, the composition of rhodocetin (subunits) in peaks *I* and *II* did not change irrespective of divalent cations during the pre-column cross-linkage. A consistent shift of peak *I* and *II* by about 10 kDa to higher apparent molecular masses was observed when rhodocetin was cross-linked in the presence of divalent cations as compared to the divalent-cation free cross-linking conditions. This indicated that only the conformation but not the quaternary structure of the rhodocetin is altered by divalent cations.

In contrast, the quaternary structure of the rhodocetin tetramer changed drastically when rhodocetin was incubated with the integrin  $\alpha 2$  A-domain prior to cross-linkage and gel filtration (Fig. 5B). To ease detection of the  $\alpha 2$  A-domain we used a YFP-tagged  $\alpha 2$  A-domain, which has an apparent molecular weight of 55 kDa and is prone to homodimerization (110 kDa) similar to the untagged  $\alpha 2$  A-domain. After incubation with rhodocetin and cross-linkage, it was detected by fluorescence at 527 nm at higher apparent molecular masses of  $165 \pm 1$ ,  $130 \pm 1$ , and  $86.5 \pm 1.7$  kDa (peaks *F-I*, *F-II*, and *F-III*, respectively) (Fig. 5B). When compared to the rhodocetin-free control, the peaks of integrin- $\alpha 2$  A-domain (peaks *F-I* and *F-III*) were shifted by about 30 - 35 kDa to higher apparent molecular masses, indicating that the YFP-tagged integrin  $\alpha 2$  A-domain was associated with a rhodocetin subunit. Interestingly, all three fluorescent peaks, *F-I* through *F-III*, contained rhodocetin  $\gamma\delta$ , but virtually no rhodocetin  $\alpha\beta$  subunit, as measured by sandwich-ELISA (Fig. 5B). The rhodocetin  $\alpha\beta$  subunit was detected at a molecular mass of  $31.2 \pm 1.9$  kDa, with a slightly lower apparent molecular mass than peak *II* in Fig. 5A of the dissociated rhodocetin subunits. This peak did not contain any rhodocetin  $\gamma\delta$  subunit and therefore contained only the rhodocetin  $\alpha\beta$  subunit. Upon integrin binding, the heterotetrameric rhodocetin dissociated, whereby its  $\gamma\delta$  subunit formed an avid complex with the  $\alpha 2$  A-domain and its  $\alpha\beta$  subunit is released. Hence, ligand binding to rhodocetin alters its quaternary structure.

### *Rhodocetin $\alpha\beta$ subunit accelerates rhodocetin $\gamma\delta$ binding to $\alpha 2$ A-domain*

Surface plasmon resonance measurement (Fig. 6) demonstrated that the rhodocetin tetramer bound to immobilized integrin  $\alpha 2$  A-domain about 280 000 times faster than the rhodocetin  $\gamma\delta$  subunit alone, whereas the rhodocetin  $\gamma\delta$  subunit alone dissociated from its integrin target several orders of magnitudes slower than the rhodocetin tetramer (Table II). While the rhodocetin  $\alpha\beta$  subunit aids in forming the complex of rhodocetin tetramer with  $\alpha 2\beta 1$  integrin, the subsequent dissociation of the rhodocetin  $\alpha\beta$  subunit renders the remaining rhodocetin  $\gamma\delta$  subunit alone with a very slowly dissociation rate, thus resulting in an almost irreversible blocking complex of rhodocetin  $\gamma\delta$  with the  $\alpha 2\beta 1$  integrin.

*Rhodocetin dissociates upon binding to cell-anchored  $\alpha 2\beta 1$  integrin*

HT1080 fibrosarcoma cells abundantly express  $\alpha 2\beta 1$  integrin. Upon incubation with rhodocetin, the HT1080 cells were decorated only with the rhodocetin  $\gamma\delta$  subunit, whereas the rhodocetin  $\alpha\beta$  subunit could not be detected on the cells by flow cytometry (Fig. 7).

Therefore, not only the isolated  $\alpha 2$  A-domain, but also cell-anchored  $\alpha 2\beta 1$  integrin induced the dissociation of rhodocetin with release of rhodocetin  $\alpha\beta$  and with firm and kinetically inert binding of rhodocetin  $\gamma\delta$  to the integrin.

## DISCUSSION:

As a natural product rhodocetin lacks any tag sequence, which usually facilitates the isolation and detection of recombinant proteins. So far, rhodocetin has to been detected by its capability to bind to  $\alpha 2\beta 1$  integrin and to inhibit collagen-induced cell adhesion. These tests were complex and impossible to perform with the crude venom because of the potential presence of contaminating cell-toxic venom components. In addition to the  $\alpha 2\beta 1$  integrin inhibition tests, we had raised a polyclonal rabbit antiserum against the rhodocetin tetramer. However, due to the high homology of the four subunits of rhodocetin [33], the fates of individual rhodocetin chains were impossible to analyse. The newly generated mAbs to the individual rhodocetin chains and their characterization have been instrumental in revealing the molecular mechanism of rhodocetin binding to  $\alpha 2\beta 1$  integrin. In this paper, we describe 11 mAbs, 9 from mouse and 2 from rat, specifically directed against different rhodocetin chains. According to their recognition pattern, they can be sorted into four groups. The first and second group recognize the rhodocetin  $\beta$  chain and the rhodocetin heterodimeric  $\alpha\beta$  subunit, respectively, whereas the third and fourth group detect an epitope within the rhodocetin  $\gamma\delta$  subunit only after or irrespective of dissociation from the rhodocetin  $\alpha\beta$  subunit, respectively. Due to their specificity, they are well suited to the detection of individual rhodocetin chains. In a newly established sandwich-ELISA, in which the mAbs are used as capturing antibodies, very low concentrations of rhodocetin chains can be quantified in the range of 0.1  $\mu\text{g/ml}$  in protein-rich samples, such as blood and urine. Hence, these mAbs might be useful in developing a fast detection assay for envenomed patients, either on the basis of the established sandwich-ELISA or even in a test-stick format. Although none of the mAbs inhibited rhodocetin binding to  $\alpha 2\beta 1$  integrin and thus will not aid in developing an effective antivenom therapy, they may help diagnostically in identifying the envenoming species. Nevertheless, generating neutralizing mAbs against venom components with low immunogenicity might be an essential and live-saving improvement in antivenom therapy [39].

In this work, the mAbs were instrumental in elucidating the changes of rhodocetin's quaternary structure and even provided evidence for conformational changes of the rhodocetin subunits, which occur upon  $\alpha 2\beta 1$  integrin binding. Interestingly, every mAb of the second group markedly increased the binding of mAbs of the first group indicating a potential conformational change within the rhodocetin  $\alpha\beta$  subunit. By contrast, only one positive interference occurred within the groups of mAbs recognizing the rhodocetin  $\gamma\delta$  subunit, as the rat mAb IC3 increased the binding signal of the murine mAb IIC9. Such conformational changes of CLRPs are not unusual and have been described for the structurally related rhodocytin/aggrexin from the same species [40] and for other heterodimeric venom CLRPs [29, 41]. However, they have never been described for heterotetrameric CLRPs in the context of subunit dissociation. Conspicuously, the mAbs against rhodocetin not only detect conformational changes of rhodocetin, but also induce its dissociation when used in immune precipitation. The mAb-induced dissociation recapitulates the changes of the quaternary

structure of the rhodocetin tetramer upon integrin binding, which can only be studied with these subunit-specific mAbs. Upon binding to the A-domain of  $\alpha 2\beta 1$  integrin, the rhodocetin subunits,  $\alpha\beta$  and  $\gamma\delta$ , dissociate, while the rhodocetin  $\gamma\delta$  subunits associates tightly with the integrin  $\alpha 2$  A-domain. From kinetic measurements, we concluded that the rhodocetin  $\alpha\beta$  subunit accelerates the binding of the rhodocetin  $\gamma\delta$  subunit to the integrin  $\alpha 2$  A-domain. After dissociation into two subunits, the rhodocetin  $\gamma\delta$  subunit remains at the integrin target with a very slow off-kinetics, thus forming an almost irreversible inhibitory complex. Moreover, with its higher solubility (data not shown), the rhodocetin  $\alpha\beta$  seems to keep the rhodocetin  $\gamma\delta$  subunit in solution until it forms the complex with  $\alpha 2\beta 1$  integrin on the cell surface. We do not yet know the newly formed interface of the rhodocetin  $\gamma\delta$ -integrin  $\alpha 2$  A-complex, but the interface between the two heterodimeric rhodocetin subunits was visualized by the crystal structure of the heterotetrameric rhodocetin [33]. The overall buried surface for the heterotetramer sums up to  $2120\text{\AA}^2$  and is comparatively small, whereby the  $\alpha$  and  $\gamma$  subunits contribute to  $\sim 80\%$  of this interface (Fig. 8). The contact between the rhodocetin subunits,  $\alpha\beta$  and  $\gamma\delta$ , is dominated by electrostatic interactions between the monomers  $\alpha$  and  $\gamma$ , respectively. The amino acid stretches, NKG<sub>76</sub>QR ( $\alpha$  chain residues 74-78) and KEQQC ( $\gamma$  chain residues 77-81), form the center of the interdomain stabilization core (Fig. 8C). Only one additional van der Waals contact (Y98 in  $\alpha$  and V94 in  $\gamma$ ) can be detected. The small interaction face with a rather low content of hydrophobic patches facilitates the dissociation of rhodocetin tetramer into two soluble subunits,  $\alpha\beta$  and  $\gamma\delta$ , with hydrophilic surfaces. This dissociation even occurred upon binding of the mAbs, and physiologically upon  $\alpha 2\beta 1$  integrin binding.

Rhodocetin is likely to share its structure prototypically with the two other known heterotetrameric CLRPs, agglucetin [42, 43] and alboaggrexin-A [44]. In their primary structure, all three CLRPs conspicuously possess a characteristic glycine residue at position 76 in their  $\alpha$  subunits with a central role in subunit interaction (Fig. 8C). Lacking the crystal structure of agglucetin and alboaggrexin-A, we can only surmise that this residue also comes to lay in the typical loop-in-the-loop motif within the subunit interface of rhodocetin [33]. No information is available so far whether agglucetin and alboaggrexin-A would dissociate into their heterodimeric subunits.

When bound to cell-anchored  $\alpha 2\beta 1$  integrin, we could not detect any rhodocetin  $\alpha\beta$  subunit bound to the  $\alpha 2\beta 1$  integrin-bearing HT1080 cells. This indicates that after binding to cellular  $\alpha 2\beta 1$  integrin, tetrameric rhodocetin undergoes integrin binding and dissociation in subsequent and very fast, or even concomitant, steps. The integrin  $\alpha 2$  A-domain is able to change its conformation upon collagen binding [3]. Although not proven for rhodocetin binding yet, rhodocetin-induced conformational changes within the A-domain might in turn lead to dissociation of the two rhodocetin subunits. In fact, conformational changes within the integrin  $\alpha 2$  A-domain are proven for EMS16, the only other crystallized,  $\alpha 2\beta 1$  integrin-inhibiting CLRP to date [45]. Binding properties of rhodocetin to integrin  $\alpha 2$  A-domain, such as the effects of divalent cations, support rhodocetin-induced conformational changes within the integrin target [34]. The crystal structure of the complex of rhodocetin  $\gamma\delta$  with the integrin  $\alpha 2$  A-domain will address this question.

The release of the rhodocetin  $\alpha\beta$  subunit after complex formation which occurs on the cell surface after envenomation prompts the question of potential functions of rhodocetin  $\alpha\beta$  subunit. In a recent paper, we demonstrated that the rhodocetin  $\alpha\beta$  subunit can bind to the platelet glycoprotein GPIIb-containing complex on platelets, thereby blocking its interaction with von Willebrand factor (vWF) [36]. Thus, tetrameric rhodocetin blocks both  $\alpha 2\beta 1$  integrin and GPIIb with its  $\gamma\delta$  and  $\alpha\beta$  subunit, respectively, thereby blocking collagen- and vWF-induced platelet aggregation much more efficiently than a venom component targeting a

single receptor only. The two other snaclecs, agglucetin [42, 43] and alboaggregin-A [44], which possess a heterotetrameric quaternary structure, block GPIIb. However, nothing is known about whether they are able to inhibit  $\alpha 2\beta 1$  integrin in a similar manner to rhodocetin. Therefore, a general molecular mechanism for heterotetrameric snaclecs similar to the one shown for rhodocetin cannot be deduced to date. The elucidation of rhodocetin's mode of action in this work explains the very effective inhibition of platelet aggregation by both collagen and vWF. To develop specific inhibitors to  $\alpha 2\beta 1$  integrin, the interaction of rhodocetin  $\gamma\delta$  subunit with the integrin requires further structural information.

#### ACKNOWLEDGEMENTS AND FUNDING:

This work was financially supported by the Deutsche Forschungsgemeinschaft through Excellence Cluster Cardio-Pulmonary System (EXC147/1) and SFB/TR23, project A8 (both J.A.E.) and the medical faculty of the University of Muenster, Germany (to L.M.S.). J.S. is a Canada Research Chair in Structural Biology and receives support from the Heart and Stroke Foundation Manitoba.

#### REFERENCES:

- 1 Santoro, S. A. and Zutter, M. M. (1995) The  $\alpha 2\beta 1$  integrin: a collagen receptor on platelets and other cells. *Thromb. Haemost.* **74**, 813-821
- 2 Barczyk, M., Carracedo, S. and Gullberg, D. (2009) Integrins. *Cell Tissue Res.*
- 3 Emsley, J., Knight, C. G., Farndale, R. W., Barnes, M. J. and C., L. R. (2000) Structural basis of collagen recognition by integrin  $\alpha 2\beta 1$ . *Cell.* **100**, 47-56
- 4 Tuckwell, D., Calderwood, D. A., Green, L. J. and Humphries, M. J. (1995) Integrin alpha2 I-domain is a binding site for collagens. *J. Cell Sci.* **108**, 1629-1637
- 5 Springer, T. A. and Wang, m. J. H. (2004) The three-dimensional structure of integrins and their ligands and conformational regulation of cell adhesion. *Adv. Protein Chem.* **68**, 29-63
- 6 Eckes, B., Zigrino, P., Kessler, D., Holtkötter, O., Shephard, P., Mauch, C. and Krieg, T. (2000) Fibroblast-matrix interactions in wound healing and fibrosis. *Matrix Biol.* **19**, 325-332
- 7 Heino, J. (2000) The collagen receptor integrins have distinct ligand recognition and signaling functions. *Matrix Biol.* **19**, 319-323
- 8 Niland, S., Westerhausen, C., Schneider, S. W., Eckes, B., Schneider, M. F. and Eble, J. A. (2011) Biofunctionalization of a generic collagenous triple helix with the  $\alpha 2\beta 1$  integrin binding sites allows molecular force measurements. *Int. J. Biochem. Cell Biol.* **in press**
- 9 Riikonen, T., Westermarck, J., Koivisto, L., Broberg, A., Kähäri, V.-M. and Heino, J. (1995) Integrin  $\alpha 2\beta 1$  is a positive regulator of collagenase (MMP-1) and collagen  $\alpha 1(I)$  gene expression. *J. Biol. Chem.* **270**, 13548-13552
- 10 Watt, F. M. (2002) Role of integrins in regulating epidermal adhesion, growth and differentiation. *EMBO J.* **21**, 3919-3926
- 11 Leitinger, B. and Hohenester, E. (2007) Mammalian collagen receptors. *Matrix Biol.* **26**, 146-155
- 12 Cosemans, M. E. M., Iserbyt, B. F., Deckmyn, H. and Heemskerk, J. W. M. (2008) Multiple ways to switch platelet integrins on and off. *J. Thromb. Haemost.* **6**, 1253-1261

- 13 Farndale, R. W., Slatter, D., Siljander, P. R.-M. and Jarvis, G. E. (2007) Platelet receptor recognition and cross-talk in collagen-induced activation of platelets. *J. Thromb. Haemost.* **5**, 220-229
- 14 He, L., Pappan, L. K., Grenache, D. G., Li, Z., Tollefson, D. M., Santoro, S. A. and Zutter, M. M. (2003) The contributions of the  $\alpha_2\beta_1$  integrin in vascular thrombosis in vivo. *Blood*. **102**, 3652-3657
- 15 Eble, J. A. (2005) Collagen-binding integrins as pharmaceutical targets. *Curr. Pharm. Design*. **11**, 867-880
- 16 Popova, S. N., Lundgren-Akerlund, E., Wiig, H. and Gullberg, D. (2007) Physiology and pathology of collagen receptors. *Acta Physiol*. **190**, 179-187
- 17 Chen, J., Diacovo, T. G., Grenache, D. G., Santoro, S. A. and Zutter, M. M. (2002) The  $\alpha_2$  integrin subunit-deficient mouse; a multifaceted phenotype including defects of branching morphogenesis and hemostasis. *Am. J. Pathol.* **161**, 337-344
- 18 Holtkötter, O., Nieswandt, B., Smyth, N., Müller, W., Hafner, M., Schulte, V., Krieg, T. and Eckes, B. (2002) Integrin  $\alpha_2$  deficient mice develop normally, are fertile, but display partially defective interaction with collagen. *J. Biol. Chem.* **277**, 10789-10794
- 19 McCall-Culbreath, K. D. and Zutter, M. M. (2008) Collagen receptor integrins: rising to the challenge. *Curr. Drug Targets*. **9**, 139-149
- 20 Nissinen, L., Pentikäinen, O. T., Jouppila, A., Käpylä, J., Ojala, M., Nieminen, J., Lipsanen, A., Lappalainen, H., Eckes, B., Johnson, M. S., Lassila, R., Marjamäki, A. and Heino, J. (2010) A small-molecule inhibitor of integrin  $\alpha_2\beta_1$  introduces a new strategy for antithrombotic therapy. *Thromb. Haemost.* **103**, 387-397
- 21 Miller, M. W., Basra, S., Kulp, D. W., Billings, P. C., Choi, S., Beavers, M. P., McCarty, O. J. T., Zou, Z., Kahn, M. L., Bennett, J. S. and DeGrado, W. F. (2009) Small-molecule inhibitors of integrin  $\alpha_2\beta_1$  that prevent pathological thrombus formation via an allosteric mechanism. *Proc. Natl. Acad. Sci. USA*. **106**, 719-724
- 22 Juárez, P., Comas, I., Gonzáles-Candelas, F. and Calvete, J. J. (2008) Evolution of snake venom disintegrins by positive Darwinian selection. *Mol. Biol. Evol.* **25**, 2391-2407
- 23 Knight, C. G., Morton, L. F., Peachey, A. R., Tuckwell, D. S., Farndale, R. W. and Barnes, M. J. (2000) The collagen-binding A-domains of integrin  $\alpha_1\beta_1$  and  $\alpha_2\beta_1$  recognize the same specific amino acid sequence, GFOGER, in native (triple-helical) collagens. *J. Biol. Chem.* **275**, 35-40
- 24 Eble, J. A. (2001) The molecular basis of integrin-extracellular matrix interactions. *Osteoarthritis and Cartilage*. **9**, S131-S140
- 25 Eble, J. A., Beermann, B., Hinz, H.-J. and Schmidt-Hederich, A. (2001)  $\alpha_2\beta_1$  integrin is not recognized by rhodocytin but is the specific high affinity target of rhodocetin, an RGD-independent disintegrin and potent inhibitor of cell adhesion to collagen. *J. Biol. Chem.* **276**, 12274-12284
- 26 Marcinkiewicz, C., Lobb, R. R., Marcinkiewicz, M. M., Daniel, J. L., Smith, J. B., Dangelmaier, C., Weinreb, P. H., Beacham, D. A. and Niewiarowski, S. (2000) Isolation and characterization of EMS16, a C-type lectin type protein from *Echis multisquamatus* venom, a potent and selective inhibitor of the  $\alpha_2\beta_1$  integrin. *Biochemistry*. **39**, 9859-9867
- 27 Staniszewska, I., Walsh, E. M., Rothman, V. L., Gaathon, A., Tuszyński, G. P., J.J., C., Lazarovici, P. and Marcinkiewicz, C. (2009) Effect of VP12 and viperistatin on inhibition of collagen receptors-dependent melanoma metastasis. *Cancer Biol. Ther.* **8**, 1507-1516
- 28 Clementson, K. J. (2010) Snake C-type lectins (snaclecs) that inhibit or activate platelets by binding to receptors. *Toxicon*. **56**, 1236-1246

- 29 Doley, R. and Kini, R. M. (2009) Protein complexes in snake venom. *Cell. Mol. Life Sci.* **66**, 2851-2871
- 30 Wang, R., Kini, R. M. and Chung, M. C. M. (1999) Rhodocetin, a novel platelet aggregation inhibitor from the venom of *Calloselasma rhodostoma* (Malayan pit viper): synergistic and noncovalent interaction between its subunits. *Biochem.* **38**, 7584-7593
- 31 Morita, T. (2005) Structures and functions of snake venom CLPs (C-type lectin-like proteins) with anticoagulant-, procoagulant- and platelet-modulating activities. *Toxicon.* **45**, 1099-1114
- 32 Paaventhana, P., Kong, C., Joseph, J. S., Chung, M. C. M. and Kolatkar, P. R. (2005) Structure of rhodocetin reveals noncovalently bound heterodimer interface. *Protein Sci.* **14**, 169-175
- 33 Eble, J. A., Niland, S., Bracht, T., Mormann, M., Peter-Katalinic, J., Pohlentz, G. and Stetefeld, J. (2009) The  $\alpha 2\beta 1$  integrin-specific antagonist rhodocetin is a cruciform, heterotetrameric molecule. *FASEB J.* **23**, 2917-2927
- 34 Eble, J. A. and Tuckwell, D. S. (2003) The  $\alpha 2\beta 1$  integrin inhibitor rhodocetin binds to the A-domain of the integrin  $\alpha 2$  subunit proximal to the collagen binding site. *Biochem. J.* **376**, 77-85
- 35 Rosenow, F., Ossig, R., Thormeyer, D., Gaßmann, P., Schlüter, K., Brunner, G., Haier, J. and Eble, J. A. (2008) Integrins as antimetastatic targets of RGD-independent snake venom components in liver metastasis. *Neoplasia.* **10**, 168-176
- 36 Navdaev, A., Lochnit, G. and Eble, J. A. (2011) The rhodocetin  $\alpha\beta$  subunit targets GPIb and inhibits von Willebrand factor-induced platelet activation. *Toxicon.* **57**, 1041-1048
- 37 Sorokin, L. M., Conzelmann, S., Ekblom, P., Battaglia, C., Aumailley, M. and Timpl, R. (1992) Monoclonal antibodies against laminin A chain fragment E3 and their effects on binding to cells and proteoglycan and on kidney development. *Exp. Cell. Res.* **201**, 137-144
- 38 Heyn, M. P. and Weischet, W. O. (1975) Circular dichroism and fluorescence studies on the binding of ligands to the  $\alpha$  subunit of tryptophan synthase. *Biochemistry.* **14**, 2447-2453
- 39 Calvete, J. J., Sanz, L., Angulo, Y., Lomonte, B. and Gutiérrez, J. M. (2009) Venoms, venomomics, antivenomics. *FEBS Letters.* **583**, 1736-1743
- 40 Watson, A. A., Eble, J. A. and O'Callaghan, C. A. (2008) Crystal structure of rhodocetin, a ligand for the platelet-activating receptor CLEC-2. *Protein Sci.* **17**, 1611-1616
- 41 Suzuki, N., Fujimoto, Z., Morita, T., Fukamizu, A. and Mizuno, H. (2005) pH-dependent structural changes at  $\text{Ca}^{2+}$ -binding sites of coagulation factor IX-binding protein. *J. Mol. Biol.* **353**, 80-87
- 42 Wang, W.-J. and Huang, T.-F. (2001) A novel tetrameric venom protein, agglutinin from *Agkistridon acutus*, acts as a glycoprotein Ib agonist. *Thromb. Haemost.* **86**, 1077-1086
- 43 Wang, W.-J., Ling, Q.-D., Liao, M.-Y. and Huang, T.-F. (2003) A tetrameric glycoprotein Ib-binding protein, agglutinin, from Formosan pit viper: structure and interaction with human platelets. *Thromb. Haemost.* **90**, 465-475
- 44 Kowalska, M. A., Tan, L., Holt, J. C., Peng, M., Karczewski, J., Calvete, J. J. and Niewiarowski, S. (1998) Alboaggregins A and B. Structure and interaction with human platelets. *Thromb. Haemost.* **79**, 609-613
- 45 Horii, K., Okuda, D., Morita, T. and Mizuno, H. (2004) Crystal structure of EMS16 in complex with integrin  $\alpha 2$ -I domain. *J. Mol. Biol.* **341**, 519-527

## TABLES:

**Table I:** K<sub>d</sub>-values of mAbs, as approximated from titration curves of immobilized rhodocetin (subunit) or rhodocetin  $\gamma\delta$ - $\alpha$ 2A-complex with the indicated mAb

mAb	Antigen	K <sub>d</sub> [nM]
VIIG2	rhodocetin $\alpha\beta$	0.85 ± 0.01
VD10	rhodocetin $\alpha\beta$	0.51 ± 0.003
IIIB6	rhodocetin $\alpha\beta$	3.34 ± 0.05
VIIIF4	rhodocetin $\alpha\beta$	4.45 ± 0.26
VIIIF9	rhodocetin $\alpha\beta$	2.05 ± 0.06
IXH7	rhodocetin tetramer, dissociated by pH-shift*	392 ± 93
IIIG5	rhodocetin tetramer, dissociated by pH-shift*	684 ± 52
VIIIB9	rhodocetin tetramer, dissociated by pH-shift*	175 ± 11
IIC9	rhodocetin tetramer	0.72 ± 0.01
	rhodocetin $\gamma\delta$ - $\alpha$ 2A domain-complex	0.59 ± 0.02
IC3	rhodocetin tetramer	20.0 ± 0.6
	rhodocetin $\gamma\delta$ - $\alpha$ 2A domain-complex	11.7 ± 0.6
ID10	rhodocetin tetramer	5.13 ± 0.04
	rhodocetin $\gamma\delta$ - $\alpha$ 2A domain-complex	6.57 ± 0.15

\* in these cases the mAb was immobilized and titrated with rhodocetin. Bound rhodocetin was detected with a rabbit antiserum against rhodocetin.

**Table II:** Kinetic association and dissociation rate constants,  $k_A$  and  $k_D$ , including standard errors (S.E.) for the interaction of rhodocetin tetramer and its  $\gamma\delta$  subunit with immobilized  $\alpha 2$  A-domain, as measured by surface plasmon resonance. The sensograms were approximated with the BIAevaluation v3.1 software, using a 1:1 Langmuir interaction model with a drifting baseline.

	$k_A$ [ $M^{-1}sec^{-1}$ ] $\pm$ S.E.		$k_D$ [ $sec^{-1}$ ] $\pm$ S.E.	
rhodocetin tetramer	$311 \times 10^3$	$\pm 0.2$	$896 \times 10^{-6}$	$\pm 0.2 \times 10^{-9}$
rhodocetin $\gamma\delta$ subunit	1.1	$\pm 8.2 \times 10^{-3}$	$1.5 \times 10^{-15}$	$\pm 1.1 \times 10^{-23}$
ratio: tetramer/ $\gamma\delta$	$280 \times 10^3$		$60 \times 10^9$	

## FIGURES:

**Fig. 1: Specificity of mAbs against rhodocetin subunits or the rhodocetin  $\gamma\delta$ -integrin  $\alpha 2$  A domain-complex**

Rhodocetin tetramer and its subunits ( $\alpha$ ,  $\beta$ ,  $\gamma\delta$ , or  $\alpha\beta$ ), as well as the integrin  $\alpha 2$  A-domain and its complex with the rhodocetin  $\gamma\delta$  subunit ( $\gamma\delta$ - $\alpha 2A$ ) were immobilized on microtiter plates at 2  $\mu\text{g/ml}$ . After washing and blocking with BSA, the wells were incubated with mAbs. Bound mAbs were detected with alkaline phosphate conjugates of anti-mouse or anti-rat IgG secondary antibodies by colorimetric conversion of *p*-nitrophenylphosphate. The binding signals were corrected for the background values measured on BSA-coated wells. Means and S.D. of quadruplet determinations are shown. According to their antigen specificity, the mAbs are sorted into four groups: The mAbs of the first group (A) bind to the isolated rhodocetin  $\beta$  subunit and to the  $\alpha\beta$  subunit to the same extent as to the entire rhodocetin. The second group-mAbs (B) recognize the  $\alpha\beta$  subunit and the entire rhodocetin, but not the isolated rhodocetin  $\alpha$  or  $\beta$  chains. The third group (C) comprise mAbs that, albeit binding with low signals, bind to the dissociated  $\gamma\delta$  subunit only, but not the rhodocetin tetramer. MAbs of the fourth group (D) detect the rhodocetin  $\gamma\delta$  subunit both as tetramer and in complex with the integrin  $\alpha 2$  A-domain.

**Fig. 2: Titration curves of the rhodocetin  $\gamma\delta$ -directed mAbs IIC9, IC3, and ID10 (A) and their effects on integrin  $\alpha 2$  A-domain binding to rhodocetin**

(A) Rhodocetin, immobilized to a microtiter plate at 2  $\mu\text{g/ml}$ , was titrated with the mAbs directed against the rhodocetin  $\gamma\delta$  subunit. Bound mAbs were quantified with an alkaline phosphatase-conjugated secondary antibody in an ELISA. Using an algorithm of Heyn and Weischet [38], the titration values, after subtraction of the background values measured in BSA-coated wells, were linearized to obtain  $K_d$  values. Based on these  $K_d$  values, the calculated titration curves are indicated with dashed lines. Every titration point was determined in duplicates. Mean values and S.D. are shown. Similarly, the  $K_d$ -values were determined for most of the mAbs against rhodocetin and are listed in Table I. (B) Binding of rhodocetin to immobilized integrin  $\alpha 2$  A-domain in the absence and presence of murine and rat mAbs IIC9, IC3, and ID10 was tested. After chemical fixation, bound rhodocetin was quantified with polyclonal rabbit antibodies against rhodocetin and an alkaline phosphatase-conjugated secondary antibody. The ELISA signals were corrected for background signals measured on BSA-coated well. Means and S.D. are shown of duplicate determinations. The titration curves were approximated similarly to the curves in (A). None of the rhodocetin  $\gamma\delta$ -targeting mAb inhibited the binding of rhodocetin to the integrin  $\alpha 2$  A-domain substantially.

**Fig. 3: Antibody interference assays**

Typical interference curves are shown of detecting mAbs which are directed against the rhodocetin  $\alpha\beta$  (A) or  $\gamma\delta$  (B) subunit. In the legend, the detecting antibody is named first, followed by the non-biotinylated interfering mAb. Means and S.D. of background-corrected and normalized binding signals of duplicate determinations are shown. Inhibitory mAbs, which had an overlapping or identical epitope to the detecting mAb, decreased the normalized binding signal with increasing concentrations. In contrast, mAbs VIIF4, VIIF9, IIIB6 (A) and IC3 (B) strongly increased the binding signals of the detecting antibodies, VD10, VIIG2 (A) and IIC9 (B), respectively. This indicated conformational changes within the rhodocetin  $\alpha\beta$  and  $\gamma\delta$  subunits, respectively, which makes the epitopes of the detecting mAbs more accessible. The mutual interference interactions of mAbs against the rhodocetin  $\alpha\beta$  and  $\gamma\delta$  are summarized in (C) and (D), respectively. The detecting mAbs are indicated in the columns, whereas the interfering mAbs are lined up in rows. Positive and negative interferences are

indicated by arrows, pointing up and down, respectively. Binding signals with IIG5 and ID10 were low (l.s. in (D)), making statements about interference impossible.

**Fig. 4: Immunoprecipitation of rhodocetin with mAbs alone (A) and in combination (B)**

Immunoprecipitation of rhodocetin from crude snake venom was carried out with the indicated mAbs against rhodocetin using protein G as pull-down agent. The mAbs were used individually (A) or in combination (B). Non-rhodocetin-directed, species-matched antibodies from mouse or rat were used (first two left lanes in A). Eluted from protein G with SDS-PAGE sample buffer and electrophoretically separated under non-reduced conditions, the precipitated rhodocetin subunits are discerned by the apparent molecular masses. The disulfide-linked rhodocetin  $\gamma\delta$  subunits runs close to 31 kDa, whereas the two chains of the  $\alpha\beta$  subunits are separated as duplet band around 14 and 16 kDa. The marker bands, 31 kDa and 14.4 kDa are indicated left of the blot. Almost all mAbs precipitated only their corresponding epitope-bearing subunit  $\alpha\beta$  or  $\gamma\delta$  subunit, indicating that they induced the dissociation of the tetrameric rhodocetin (A). As exception, the three mAbs IXH7, VIII B9, and IIG5 did not pull down the  $\gamma\delta$  subunit at all (A), unless the precipitation was performed in the presence of one of the dissociation-inducing mAb VIIG2 (B).

**Fig. 5: Gel filtration of cross-linked mixtures of rhodocetin alone (A) or with YFP-tagged  $\alpha 2$  A-domain (B)**

Either alone (A) or together with YFP- $\alpha 2$  A-domain (B), rhodocetin was incubated and cross-linked with BS3. The mixtures were separated according to their molecular masses on the calibrated TSK 2000 column. The masses of the calibration marker proteins are indicated by vertical grid-lines. The protein content of the eluate was assessed by optical density at 219 nm (OD(219nm), solid grey line) and by fluorescence emission at 527 nm (em.(527nm), dashed gray line), both as right y-axes. The fluorescence detected the YFP-tagged integrin  $\alpha 2$  A-domain in three peaks, labelled *F-I* through *F-III* (B), whereas rhodocetin alone showed two major peaks, *I* and *II*, the former one with a higher molecular mass-shoulder (A). The eluate fractions were scrutinized for the contents of rhodocetin subunits,  $\alpha\beta$  (open circles) and  $\gamma\delta$  (grey squares), in a sandwich-ELISA, indicated as OD(405nm)-values and shown as left y-axis. Means and S.D. of duplicate determinations in the sandwich-ELISA are shown.

**Fig. 6: Surface plasmon resonance-based measurement of rhodocetin tetramer (A) and  $\gamma\delta$  subunit (B) interaction with the integrin  $\alpha 2$  A-domain.**

Binding of rhodocetin tetramers (A) and its  $\gamma\delta$  subunit (B) to CM5 chip-immobilized integrin  $\alpha 2$  A-domain was monitored as sensograms in the BiaCore X in real time. Correspondingly diluted buffer values were measured for the rhodocetin  $\gamma\delta$  solutions (in B) and subtracted from the sensograms. Kinetic data were evaluated by using a 1:1 Langmuir interaction model and are shown in Table II.

**Fig. 7: Flow cytometric analysis of rhodocetin interaction with  $\alpha 2\beta 1$  integrin-bearing HT1080 fibrosarcoma cells**

The murine (left panels) and rat (rat panels) antibodies were used to detect bound rhodocetin subunits on the membrane-anchored  $\alpha 2\beta 1$  integrin of HT1080 fibrosarcoma cells. Whereas the  $\alpha\beta$  subunit-detecting mAbs, VIIG2 and VD10, did not bind to rhodocetin-treated cells, the rhodocetin  $\gamma\delta$  was bound to  $\alpha 2\beta 1$  integrin on the cell surface, as detected with the corresponding mAbs, IIC9, IC3, and ID10.

**Fig. 8: Interface between the subunits,  $\alpha\beta$  and  $\gamma\delta$ , of the rhodocetin tetramer.**

(A) and (B) The crystal structure of the rhodocetin tetramer with the subunits,  $\alpha$  (red),  $\beta$  (green),  $\gamma$  (blue) and  $\delta$  (yellow). The surfaces of the two subunits,  $\alpha$  and  $\gamma$ , and the interface (dark red and blue) are shown from two different angles (A and B). In (C), the interface is shown in detail. Two potential electrostatic interactions pairs, E $\alpha$ 92-K $\gamma$ 77 and R $\alpha$ 78-E $\gamma$ 78, and one van der Waals contact, Y $\alpha$ 98-V $\gamma$ 94, are likely to hold the subunits together. The side chains of the residues K $\gamma$ 77 and E $\gamma$ 78 form a cleft, through which only the side chain-less glycine residue, G $\alpha$ 76, of the  $\alpha$  chain fits. The subunit interface spans a comparatively small area. Moreover, dissociation of this interface renders the surfaces of both subunits with charged and hydrophilic residues, providing two individual and soluble entities,  $\alpha\beta$  and  $\gamma\delta$ . The pictures were generated with DINO (<http://www.dino3d.org>).

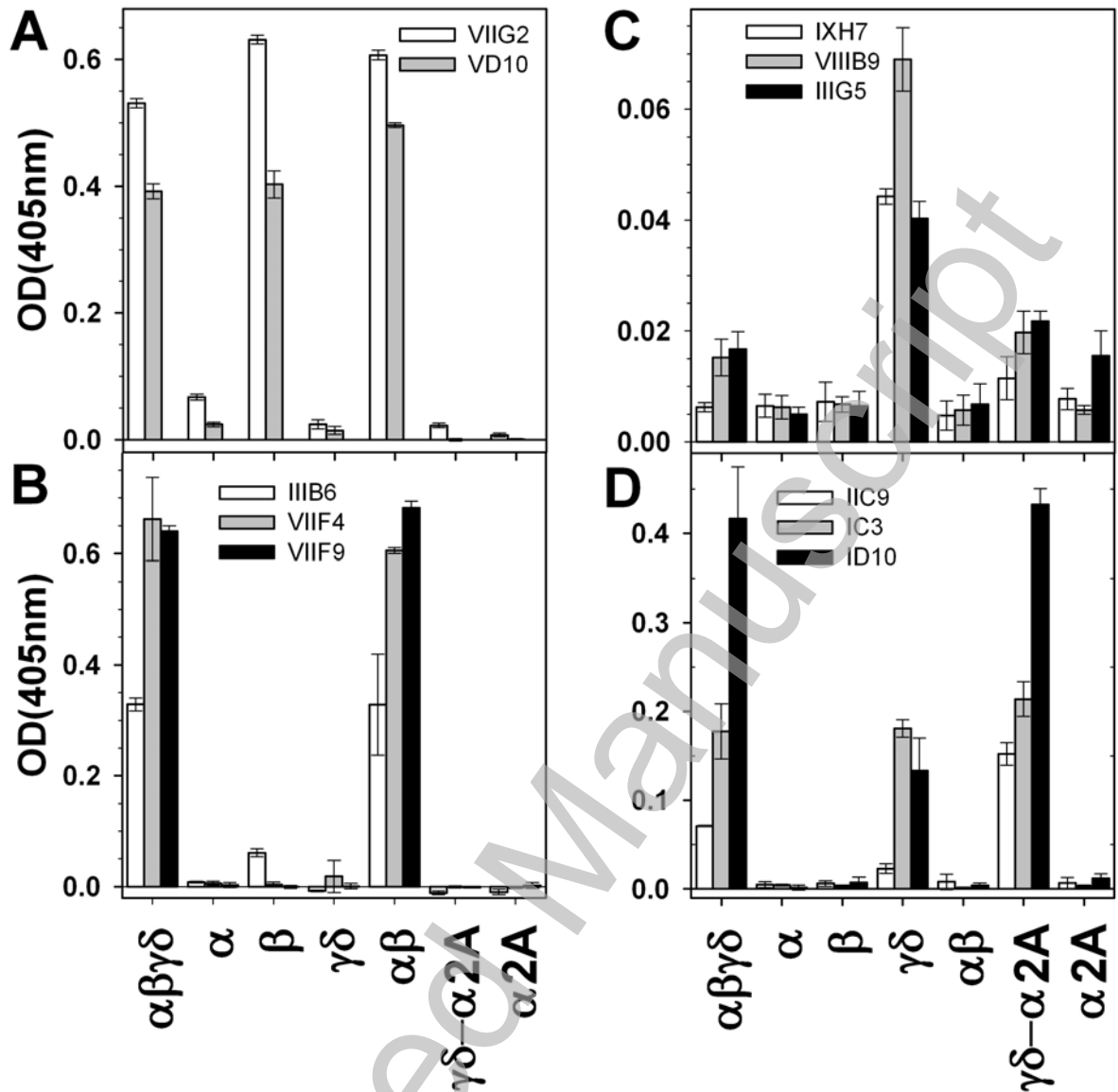
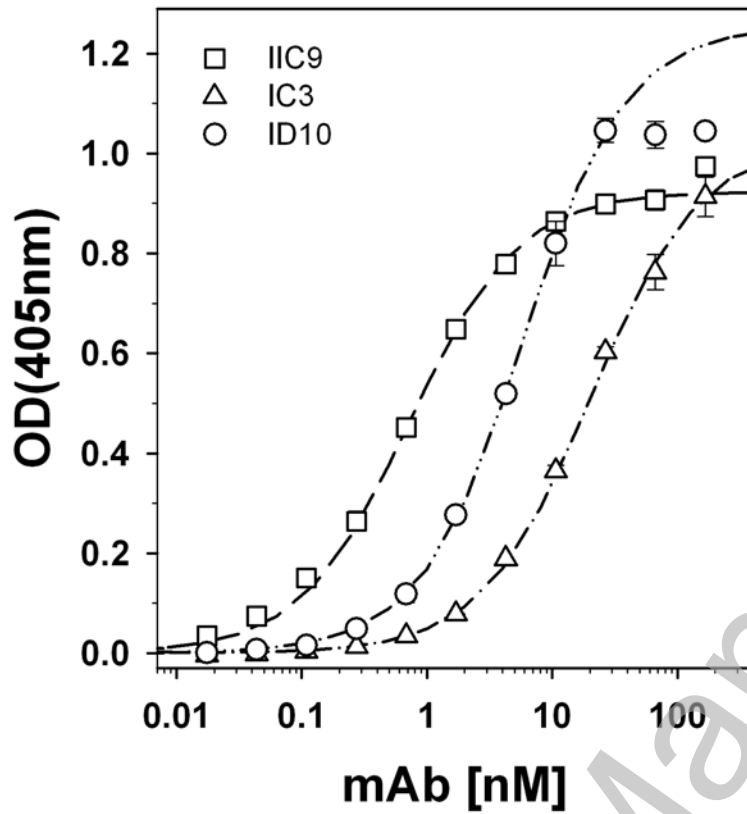


Fig. 1

THIS IS NOT THE VERSION OF RECORD - see doi:10.1042/BJ20110584

**A**



**B**

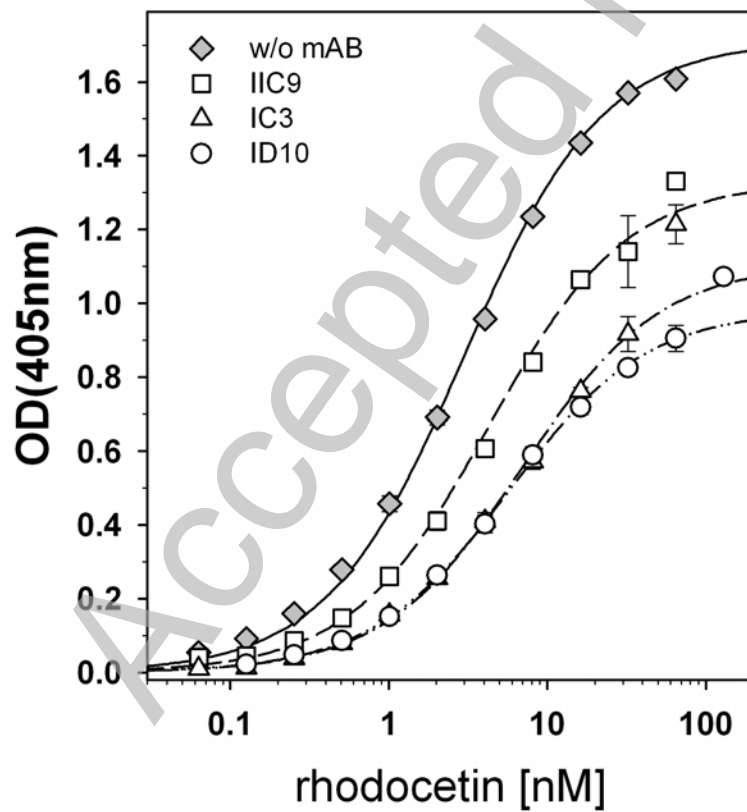
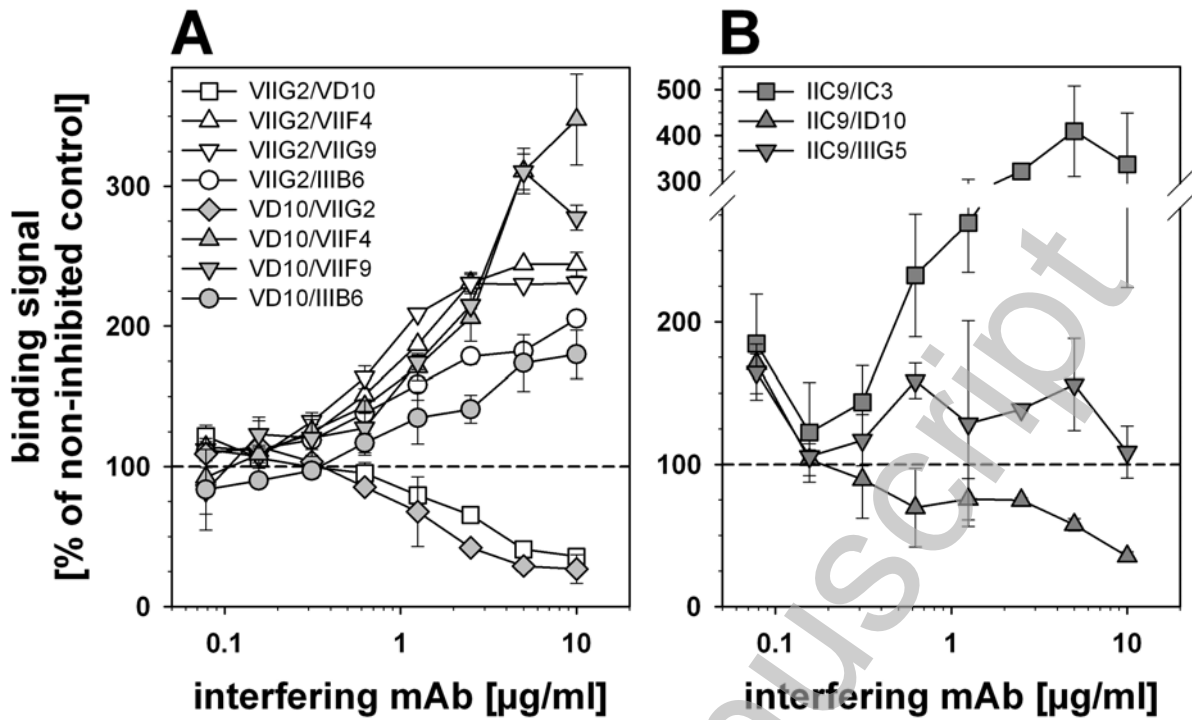


Fig. 2

THIS IS NOT THE VERSION OF RECORD - see doi:10.1042/BJ20110584



**C** Rhodocetin  $\alpha\beta$  Dimer

		detecting mAb				
		VII G2	V D10	III B6	VII F4	VII F9
interfering mAb	VII G2	X	↓			
	V D10	↓	X			
	III B6	↑	↑	X		
	VII F4	↑	↑	↑	X	↓
	VII F9	↑	↑	↑	↓	X

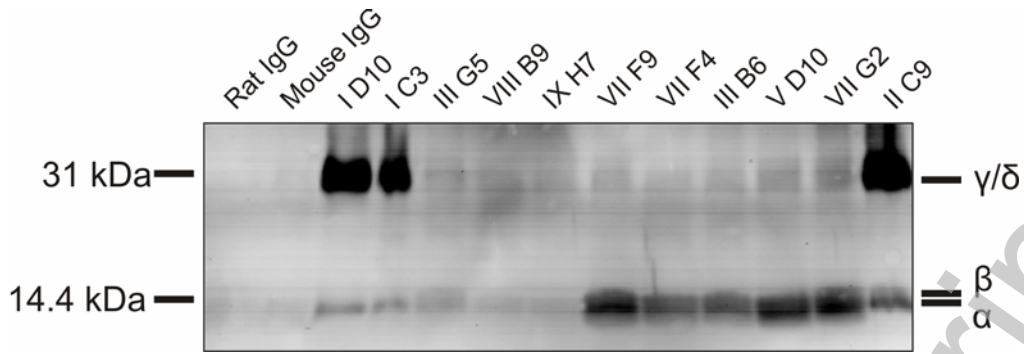
**D** Rhodocetin  $\gamma\delta$  Dimer

		detecting mAb					
		IX H7	VIII B9	III G5	II C9	I C3	I D10
interfering mAb	IX H7	X	↓	l.s.			l.s.
	VIII B9	↓	X	l.s.			l.s.
	III G5			X			l.s.
	II C9			l.s.	X		l.s.
	I C3			l.s.	↑	X	l.s.
	I D10			l.s.	↓		X

Fig. 3

THIS IS NOT THE VERSION OF RECORD - see doi:10.1042/BJ20110584

**A**



**B**

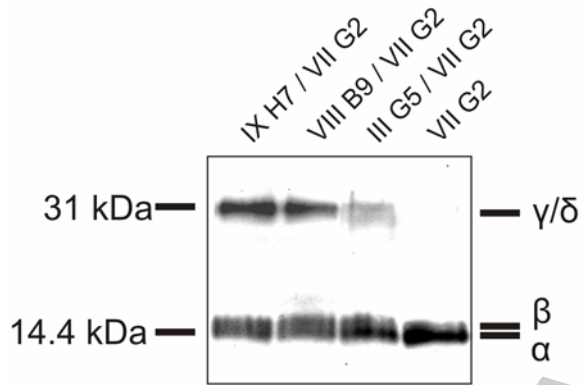


Fig. 4

THIS IS NOT THE VERSION OF RECORD - see doi:10.1042/BJ20110584

Accepted Manuscript

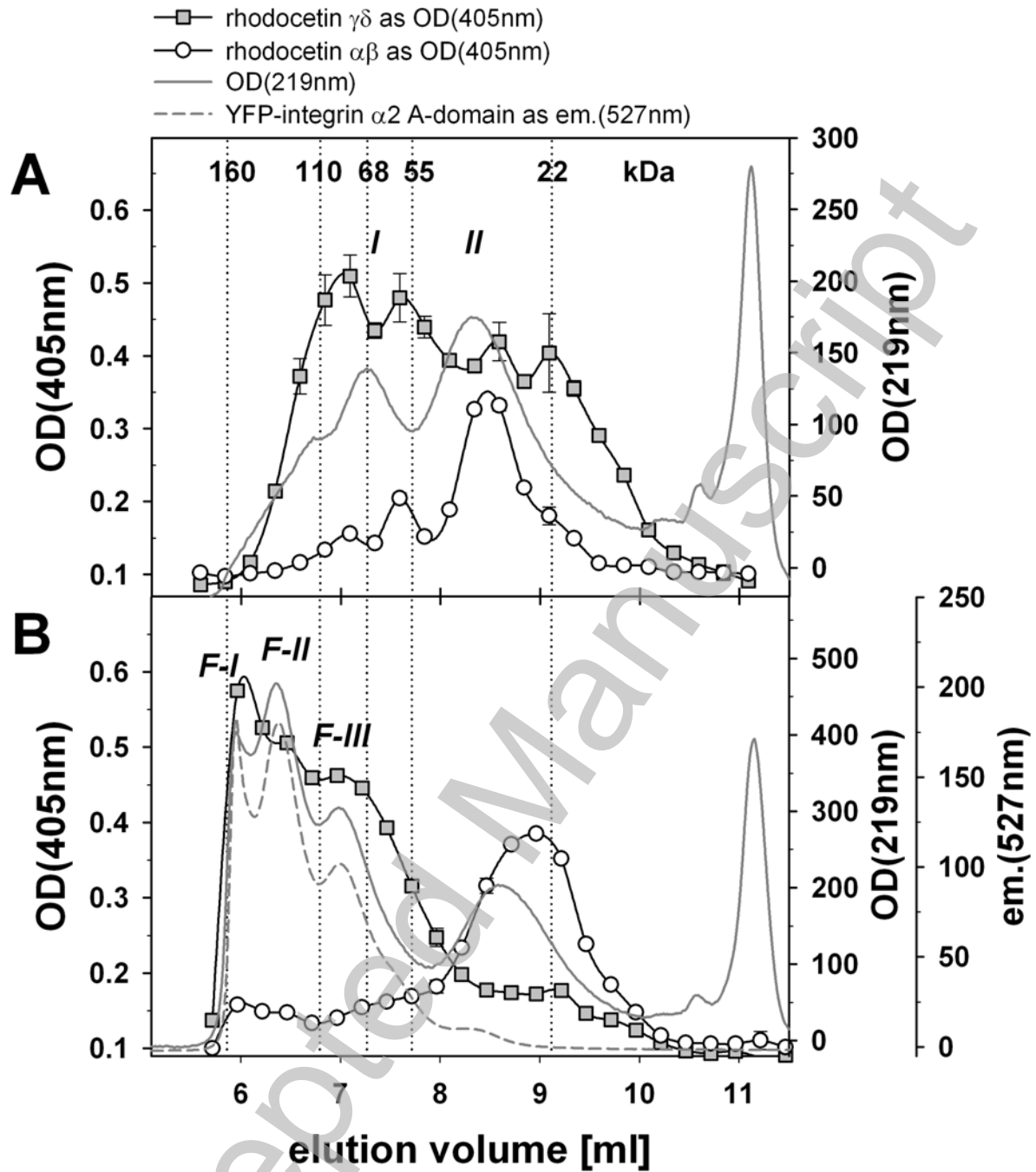


Fig. 5

THIS IS NOT THE VERSION OF RECORD - see doi:10.1042/BJ20110584

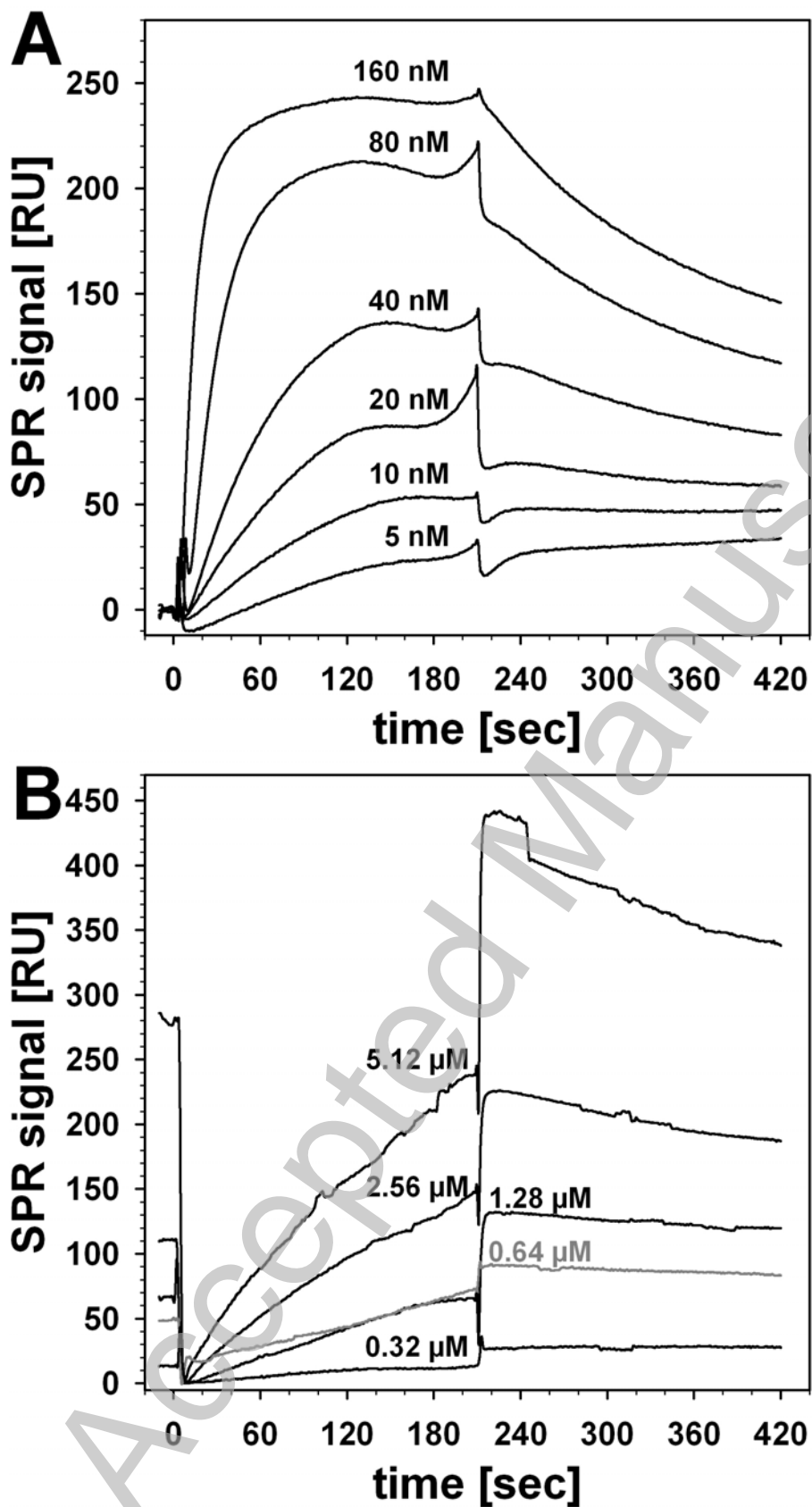


Fig. 6

THIS IS NOT THE VERSION OF RECORD - see doi:10.1042/BJ20110584

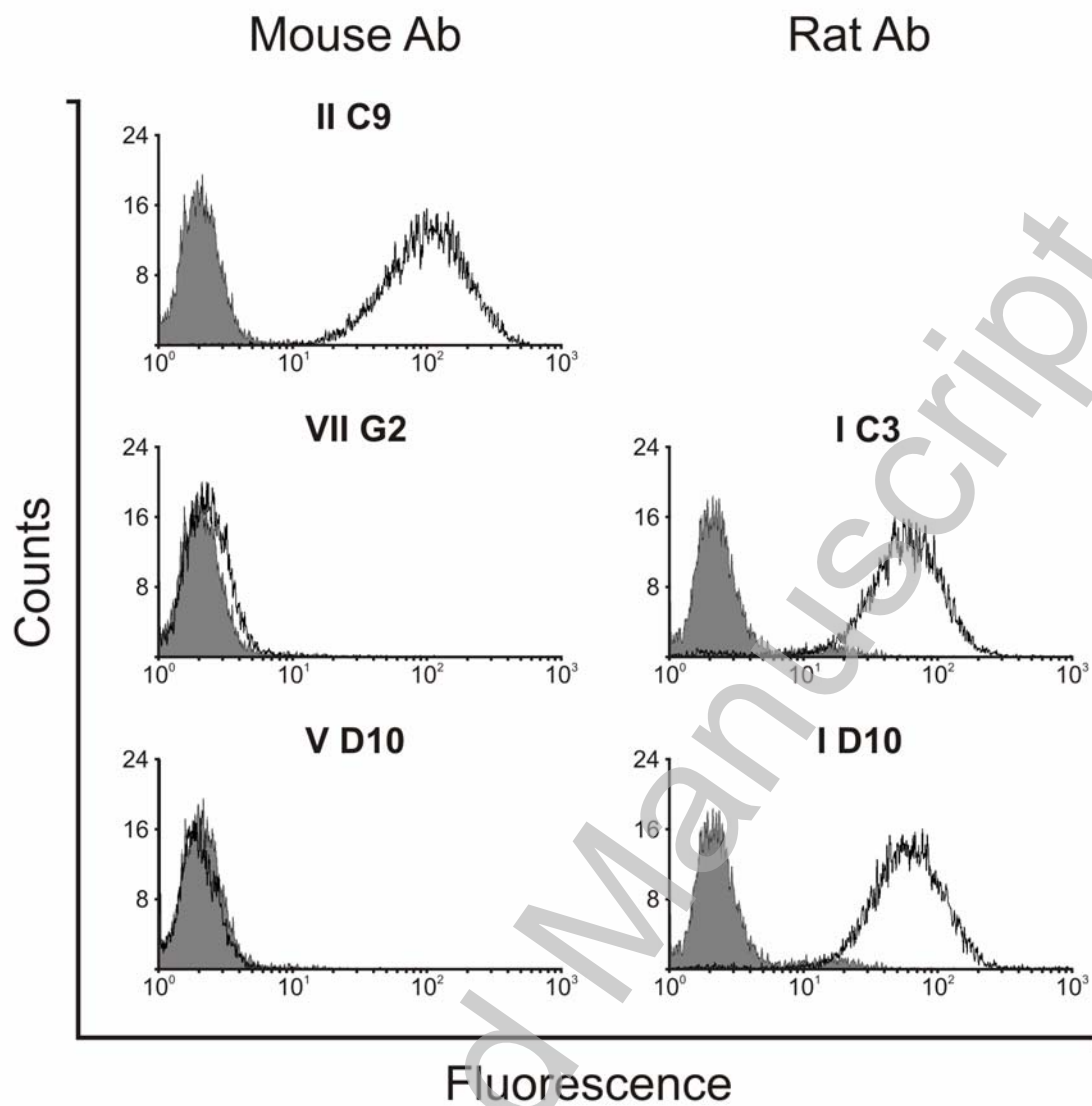


Fig. 7

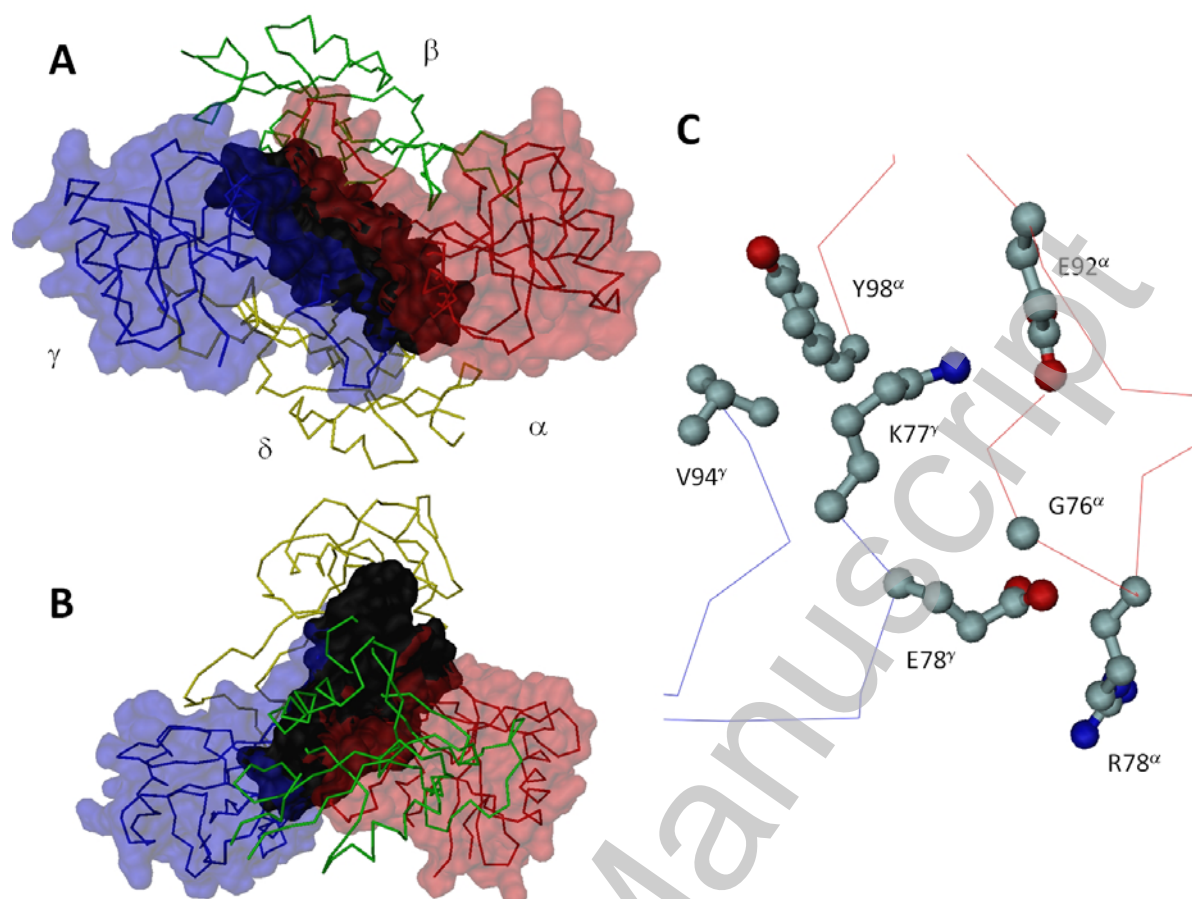


Fig. 8